Identifying Weaknesses in AC Shipboard Power Systems Operation during Motor Starts and Reacceleration

V. C. Nikolaidis, K. Z. Ioannidis, J. M. Prousalidis

***Abstract*--This paper analyzes the dynamic behavior of an actual AC shipboard power system with a significant number of induction motors. As part of this work, a typical overcurrent protection system for this system is designed as well. Dynamic simulation runs including motor starting procedures are conducted. These scenarios consider the application of different motor starting methods and motor starting time sequences. Moreover, dynamic transitions from one operational state of the ship to another are simulated. During these transitions motor loads and static consumption changes are studied. The simulation results highlight the need to intensively focus on motor starting and protection systems when designing and operating a ship.**

***Keywords*: Induction motors, motor reacceleration, motor starting, shipboard power systems, voltage dips.**

I. Introduction

CONVENTIONAL alternative-current (AC) shipboard power systems can be characterized as complete, autonomous, radial power grids, consisting of power generation, distribution, and utilization [1]. One key feature of onboard electrical installations is the close distance between all the installed system components, as the total power capacity can reach 40-80 MW in an area of just a few square meters and a typical length of distribution cables between 50-1000 m.

The majority of AC shipboard power systems consists of a wide variety of induction motors, numerous static consumptions, and a few special loads (radar etc.). The existence of a significant number of induction motors on an autonomous power system, makes examining motor starting related dynamic phenomena very important. Especially, voltage dips during motor starts are critical and have unique characteristics due to the unique shipboard power system features [2]-[4]. Many ship accidents have been attributed to power quality issues, like voltage dips [5].

A prediction method of voltage dips caused by heavy motor starts in AC ships is proposed in [6]. In this work, the impact of motor starts is estimated based on the Riemann-summation-principle evaluation method. Both balanced and unbalanced voltage condition are considered, however only individual motor starts are assumed. The research work [7] proposes adopting an inverter-coupled energy storage system as a soft-starting mechanism to control motor load starting currents and voltage response during post-fault system restoration. Although this method is efficient, it requires a rather complex control logic. A shunt and a series compensation device are proposed in [8] and [9] respectively, but this solution assumes installing an expensive device only for that purpose.

This paper focuses on more common motor starting solutions using a star-delta switch, an autotransformer or a variable resistance set, which reduce the motor terminal voltage for a short time and then supply the full voltage value. The impact of these motor starting procedures on voltage response of a shipboard power system is examined. Moreover, the interaction of motor starts and reacceleration with the overcurrent protection system is investigated. The organization of this paper is as follows. Section II describes the electrical system of the tanker ship under investigation, as well as the modelling approach for the power system and protection equipment. In Section III, the distinct operating states of the ship are addressed. Section IV describes all the simulated motor starting cases and procedures, whereas the simulation results are illustrated in Section V. Conclusions of this work are drawn in Section VI.

II. Shipboard Power System

A. Description

Fig. 1 shows the simplified model of the AC power system of the real tanker ship under investigation. Two out of three identical 4-pole, 440 V, 1200 kVA (960 kW), 60 Hz synchronous diesel generators supply the loads, which in majority are connected directly to the 440 V distribution network. The third generator is held in a standby offline mode in case of an emergency. A small number of 220 V loads (i.e. the aggregated static load GL and motor M15) are fed through a 440/220 V, 100 kVA, Dd0, 60 Hz step-down transformer. Twelve XLPE, single-core and multi-core cable feeders of various conductor sizes and parallel circuits connect all the components together.

The total system load consumption varies depending on the operation state of the ship. The latter determines which loads

V. C. Nikolaidis is with the Department of Electrical and Computer Engineering, Democritus University of Thrace, Xanthi 67100, Greece (e-mail: vnikolai@ee.duth.gr).

K. Z. Ioannidis is with Akuo Energy, Athens, Greece (e-mail: konsioan1@gmail.com).

J. M. Prousalidis is with the School of School of Naval Architecture and Marine Engineering, National Technical University of Athens, Athens, Greece (jprousal@naval.ntua.gr).

Paper submitted to the International Conference on Power Systems Transients (IPST2021) in Belo Horizonte, Brazil June 6-10, 2021.

are in operation and their actual consumption as a percentage of their rated power.

B. System Modelling

The shipboard power system under examination has been modelled with the use of the PowerFactory software. The detailed synchronous machine model 2.1 is adopted for the representation of the diesel generators [10]. Each generating unit is supplemented by a simplified automatic voltage regulator (AVR), which is represented with the well-known SEXS model [11]. Moreover, the detailed model DEGOV1 [11] is used to represent the governor of each generating unit. Typical parameters have been used for the AVRs and the governors.

In order to simplify the system model, but without sacrificing the accuracy of their dynamic response in the simulations, motor loads are adequately aggregated. Specifically, motors that are connected at the same bus and have a power rating that is lower than 100 kW, are grouped together to create an equivalent induction motor. On the other hand, induction motors with a higher power rating are modelled individually. The aforementioned procedure results in fifteen induction motors (namely M1-M15).

Based on the rated power data of the fifteen induction motors, as well as on their inertia/torque class and usage, these motors are categorized in seven motor categories A-G (Table I). For each motor category, a specific speed-torque characteristic is assigned that is representative to the operation characteristics of all motors in this category. Then, for each motor belonging to a specific category, a parameter estimation procedure is followed [12], to determine the parameters of the motor circuit model. The classical induction machine model with a frequency (or slip) dependent rotor impedance is adopted for the representation of all motors. As for the rotor circuit, single and double cage models with current displacement are adopted [13].

The passive loads are grouped together to form an aggregated constant power load (GL). Special loads (radars etc.) are treated as static loads and therefore they have been included in the constant power load GL.

The pi-equivalent model is used for the representation of the cable feeders. Cables' routing and installation method is taken into account to determine the derating factor of each cable circuit.

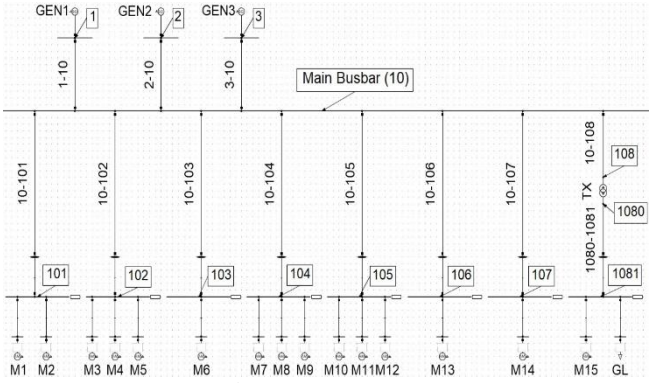

Fig. 1. One-line diagram of the examined system.

TABLE I
MOTOR CATEGORIES

Motor Category	Included Tanker Grid Motors	Rated Power (kW)	Starting torque (pu)	Moment of Inertia ($kg \cdot m^2$)
A	M1,M3,M8,M9,M13,M14	120	1.40	1.21
B	M2	375	1.50	4.20
C	M4,M5	440	1.70	4.50
D	M6,M12	44	1.90	0.15
E	M7,M11	90	2.00	0.65
F	M10	145	1.40	1.44
G (220V)	M15	9	0.46	0.0168

C. Protection Modelling

Motors, transformers, and feeders are protected by low-voltage molded-case circuit-breakers (MCCBs) of various vendors, with an inverse-time thermal element and definite-time and/or instantaneous magnetic elements. The rating of their trip unit is selected depending on the breaking capability required at the place of installation.

The generators are protected by numerical multifunctional protection relays. Differential protection and other protective functions (e.g. reverse power, underfrequency, etc.), although extremely important for the generator protection, they are not critical from the viewpoint of dynamic voltage response. The undervoltage element of the generator relay is used to detect loss-of-voltage conditions (terminal voltage in the order of 35%-50%) and therefore it does not play actual role in the simulations as well. Hence, for the purposes of this paper, only the generator overcurrent elements are of interest. A voltage-restrained inverse-time overcurrent element and two definite-time/instantaneous overcurrent elements are in use.

It must be noted that although the type of the protection equipment used in the grid is known, the settings of the relays are not given. For this reason, a complete protection coordination study has been conducted to determine appropriate pickup (PU) and time-dial (TD) settings for the MCCBs and the generator voltage-restrained overcurrent elements, so that selectivity is achieved throughout the grid. In this selectivity study, possible operating states and configurations of the electrical system have been considered to determine the critical pre-fault load-flow conditions. Moreover, other critical issues affecting protection operation, such as motor starting currents, transformer inrush currents, damage curves etc. have been also examined in the study.

It is understood that for the protection coordination study all MCCBs and relays are represented in the PowerFactory software model by using appropriate protection models found in the program library. A typical protection selectivity example is shown in Fig. 2. In this time-overcurrent graph retrieved from the program, the solid curve corresponds to the M2 motor starting characteristics. The dashed curve corresponds to the time-overcurrent settings of the MCCB protecting motor M2, whereas the dotted curve corresponds to the time-overcurrent settings of the incoming feeder protection. In the same graph, the voltage-restrained overcurrent element curve of generator G1 is depicted with dashed-dotted line. Similar time-overcurrent graphs hold for every motor-feeder-generator path.

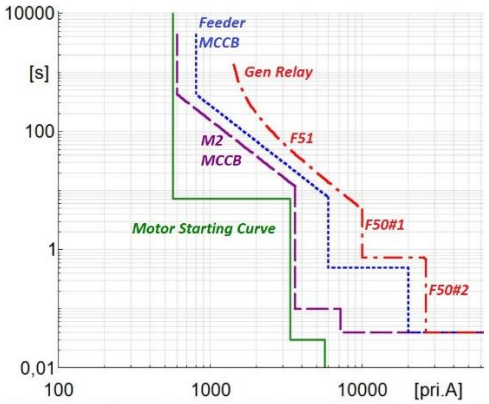

Fig. 2. Example of overcurrent protection coordination.

TABLE II
MOTORS LOADING PER OPERATIONAL STATE (IN KW)

Motors	NCS	MS	ASS	LS	US
M1	**110.92**	90.13	-	-	-
M2	119.22	**341.77**	97.09	97.09	97.09
M3	**86.05**	-	-	-	-
M4	-	-	-	401.28	401.28
M5	**430.94**	404.63	243.59	305.60	330.51
M6	17.40	-	32.83	**34.23**	33.05
M7	74.34	74.34	74.34	74.34	74.34
M8	97.87	-	-	97.87	-
M9	101.02	101.02	101.02	101.02	101.02
M10	-	**126.38**	-	-	-
M11	-	**84.26**	-	-	-
M12	-	-	**35.25**	31.43	31.43
M13	**94.51**	80.40	38.08	66.29	66.29
M14	112.00	112.00	112.00	112.00	112.00
M15	7.5	7.5	7.5	7.5	7.5
Total	1251.77	**1422.43**	741.70	1328.65	1254.51

III. SYSTEM OPERATION STATES

The total load power demand is not constant as it is directly related to the operational state of the tanker. For instance, there are operation states where several motors are out of operation, whereas in other states the loading of the motors is changed. This aspect is one of the naval crafts main characteristics and leads to the need of clear identification of the different operational states in order to simulate the grid under all possible conditions.

Five possible operational states are identified for the tanker ship under investigation:

- *Normal Cruising State* (NCS): Cruising in open sea with steady speed and course.
- *Maneuvering State* (MS): Navigation with maneuverings, course and speed changes.
- *Anchor-Standby State* (ASS): Anchored at harbor.
- *Loading State* (LS): During in port cargo loading procedures.
- *Unloading State* (US): During in port cargo unloading procedures.

LS and US share many similarities but are considered as two separate states because of some differences on the total power demand.

Table II summarizes the motors loading level related to the abovementioned ship operation states. The most demanding operational state in terms of total power is the MS with a total power demand equal to 1422.43 kW. Nevertheless, each motor experiences maximum loading in different states (marked in bold), whereas in some cases motor load remains unaffected during the transition between states. The latter is observed in motors M7, M9, M14, M15, which drive crucial loads that must constantly be supplied.

IV. SIMULATED STARTING PROCEDURES

The scope of this work is to analyze the dynamic voltage response of the examined electrical system during individual motor starts and motor reacceleration caused by transitions from one operational state to another. Possible interaction with the protection system operation is also investigated.

In this context, the simulation analysis includes three different groups of scenarios:

- *Group 1 of Scenarios* (G1oS): Individual motor starts.
- *Group 2 of Scenarios* (G2oS): Sequential motor starts.
- *Group 3 of Scenarios* (G3oS): Transition between the different operational states.

A. Group 1 of Scenarios

This first group of scenarios concerns the simulation of the starting (acceleration) phase of each individual motor (M1-M15). In these simulations, it is assumed that each motor drives the total (100%) of the coupled mechanical load during the starting phase, to examine the largest voltage dip cases.

Four different starting methods are considered in the simulations:

- *Direct-on-line starting* (DOL): The motor starts being directly connected to the grid. No additional starting equipment is used.
- *Starting with star-delta switch* (Y-D): The motor starts being initially on star connection with the grid. After some time, the motor supply switches to a delta connection. The adequate switching time is related with the speed of the rotor. In this work, it is assumed that the switching from star to delta connection occurs when the rotor speed reaches the value of 0.6 pu.
- *Starting with variable resistance* (VR): The motor starts initially with a variable resistance connected to the rotor circuit. During the acceleration phase, the resistance is gradually or stepwise removed until the rotor reaches its nominal speed. In this work, resistance removal occurs twice, when the rotor speed reaches the values of 0.3 pu and 0.7 pu.
- *Starting with auto-transformer* (ATF): The motor starts with the help of an autotransformer that initially provides reduced voltage level which is gradually restored to 100% until the motor reaches its nominal speed. In this work, voltage increases in two steps, when the rotor speed reaches the values of 0.25 pu and 0.5 pu.

Based on the simulation results, the best starting method is adopted for each motor in terms of voltage and current response. Obviously, the starting method causing the smallest possible voltage dip/overcurrent or an acceptable undervoltage/overcurrent combination during the start of each individual motor is selected. The required additional equipment and installation costs are not considered in this

decision. Once the best (suboptimal) starting method is selected for each motor, this will be considered hereafter as the default starting option of this motor in the G2oS and G3oS.

B. Group 2 of Scenarios

The second group of scenarios concerns the simulation of sequential motor starts as a black-start procedure. Specifically, in these scenarios the system is considered originally unloaded (all motors and loads are disconnected) but energized, when gradually motors begin to start until the system transits to one of the operational states mentioned in Section III. The transition is achieved in two different ways:

- *Sequence 1*: A motor is started, only if the previously started motor has already reached its nominal speed. For comparison, this investigation is performed twice:
  a) Considering the best starting option for each motor (derived from G1oS)
  b) Considering DOL motor starts.
- *Sequence 2:* In this case, the motor starting procedure is based on a predefined program:
  a) Each motor control centre (MCC) (i.e. the buses 101-107 and 1081) is energized following a coordinated time sequence. That is that at the time a MCC is energized, the previously started motor(s) (i.e. that supplied from different MCCs) have already reached nominal speed. However, when multiple motors are connected to the same MCC, they will start simultaneously upon MCC energization.
  b) MCCs are energized based on a predefined schedule but without waiting for the previously started motors (i.e. at different MCCs) to reach steady state. A time-coordinated start holds only for motors supplied from the same MCC.

C. Group 3 of Scenarios

This group of scenarios concerns the simulation of the transition from one operational state to another. Five separate transitions have been simulated:

a. From the MS to the NCS.
b. From the NCS to the MS.
c. From the ASS to the NCS.
d. From the ASS to the LS.
e. From the ASS to the US.

These transitions can be regarded as the most common and often observed as, in simple terms, describe the potential dynamic changes in the handling of the tanker in the open sea and in the harbor. During these transitions, a number of motors is being disconnected, whereas other moves to a different loading state (reacceleration).

V. Simulation Results

A. Individual Motor Start (G1oS)

An indicative example out of all the simulation results of the G1oS is described in this subsection. Specifically, the starting of the motor M2 is illustrated below. Note that this occurs when the ship is operating in the MS, where the M2 motor loading is maximum (341.77 kW).

Fig. 3 depicts the absorbed current variation during the starting of motor M2. The different curves correspond to one of the examined starting methods. Obviously, the starting method affects the current magnitude, as well as the time until the motor reaches its nominal speed. The DOL approach causes the highest current during the motor acceleration phase, whereas the VR has the smallest impact.

In the same figure, the minimum pickup current of the inverse-time, the definite-time and instantaneous overcurrent element of the MCCB protecting motor M2 is shown. In all the starting cases, the inverse-time overcurrent element picks-up. Nevertheless, because of the limited duration of the inverse-time pickup current violation, the MCCB never trips the motor circuit breaker.

Fig. 4 depicts the voltage magnitude of the main bus during the start of motor M2. In the same figure, two different voltage thresholds are shown. These thresholds correspond to the minimum allowed voltage magnitude in naval power grids, according to the regulation of the Germanischer Lloyd [14]. In particular, the voltage magnitude may drop down to 0.9 pu for permanent operation, and down to 0.8 pu for less than 1.5 s under emergency situations.

It can be concluded from Fig. 4 that the DOL starting of M2 violates the 0.8 pu limit for more than 1.5 s. Therefore, DOL starting is prohibited for M2. The voltage drop is significantly reduced with the addition of VR or the use of Y-D switch and ATF. Overall, the use of VR is chosen as the best starting method for M2. The same is true for all motors of the Category B.

The highest rated (440 kW) motor M5 must be given special attention. Specifically, if the high-power output of 430.94 kW (corresponding to the NCS of the ship) is demanded during the start of M5, this leads to a high absorbed current (above nominal – see Fig. 5) and causes a voltage collapse at the main bus voltage (see Fig. 6). Normally, the motor will be tripped by the protection.

The latter detrimental effect is avoided only when a VR is used as a starting method for motor M5. Consequently, the use of VR is considered as the best starting method for motor M5. The same is true for all motors of the category C.

The motors with lower rated power output, belonging to the categories A, D, E, F, G, do not show prohibited voltage drops and overcurrents when started DOL. As a result, the DOL starting method is adopted for those motors.

Conclusively, the starting method applied to each motor in the G2oS and G3oS is:

- DOL for motors belonging in categories A, D, E, F, G.
- VR for motor belonging in categories B and C.

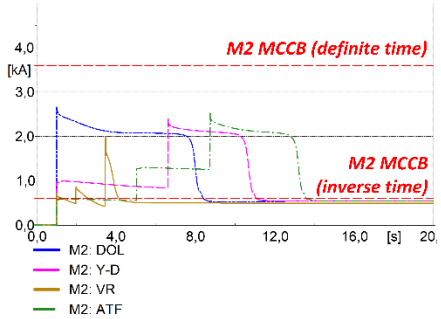

Fig. 3. Current input of motor M2.

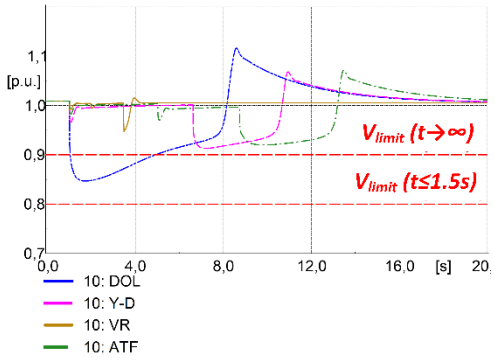

Fig. 4. Main bus voltage response during the start of M2.

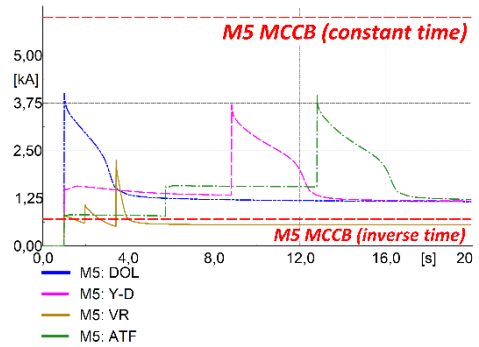

Fig. 5. Current input of motor M5.

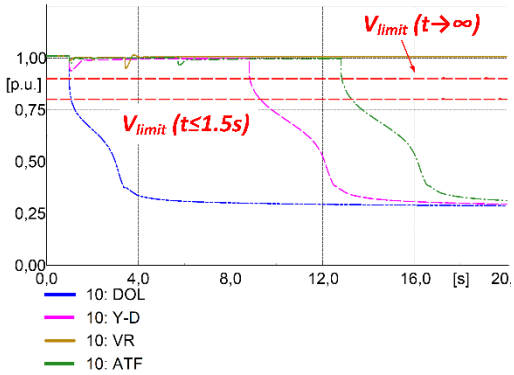

Fig. 6. Main bus voltage response during the start of M5.

B. Sequential Motor Start (G2oS)

The first indicative example from the G2oS is the simulation of the motor starting plan sequence 1, shown in Table III. This motor starting plan ends when the ASS is achieved. Note that sequence 1 assumes that a motor starts only if the previously started one has reached nominal speed.

Fig. 7 illustrates the response of the main bus voltage magnitude during the simulation of the aforementioned motor starting sequence. No prohibited voltage violation is observed. If, however, all motors (meaning M2 and M5 as well) started DOL in this scenario, voltage would collapse as can be seen with the dashed-dotted line in Fig. 7.

Fig. 8 illustrates the current output of one generator during the simulation of this scenario. The same current output holds for the second generator in operation since they are identical. As can be seen, when the DOL starting method is applied to all motors started based on sequence 1, the generator voltage-restraint overcurrent element picks-up and it will trip the unit after some seconds. This is not true if motors M2 and M5 start with VR. A slight violation of the pickup current is again observed in the latter case, but it does not last as much as needed for tripping the generating unit.

The second example from the G2oS is the simulation of the motor starting sequence 2a. In this example, the motors start based on the plan shown in Table IV. That means that individual motors start in distinct time steps (shown in Table IV), allowing the previously started motor to accelerate up to its to nominal speed. At time t = 40 s, motors M7 and M9 (connected to the bus 104) are starting simultaneously. This results to an extensive motor starting current in the feeder 10-104 that exceeds the current pick-up setting of the feeder MCCB (Fig. 9). As a consequence, the feeder circuit breaker is tripped and both motors are disconnected from the network. Hence, the finally desired ASS of the ship cannot be achieved.

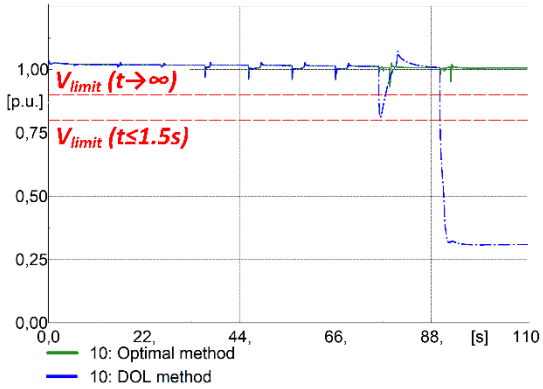

Fig. 7. Main bus voltage response during the motor start sequence 1.

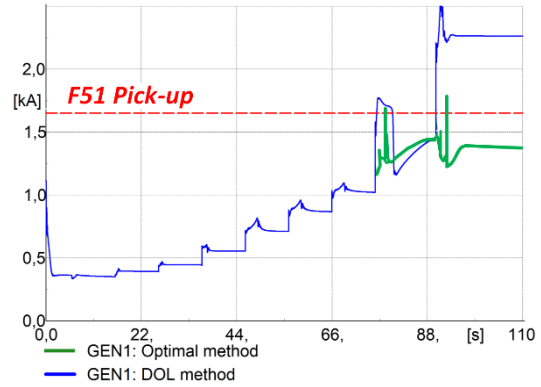

Fig. 8. Generator current output during the motor start sequence 1.

TABLE III
MOTOR STARTING PLAN SEQUENCE 1

Motors-Loads	Connection Moment t (s)	Starting Method
Load (GL)	1	Connected
M15	6	DOL
M12	16	DOL
M6	26	DOL
M7	36	DOL
M9	46	DOL
M14	56	DOL
M13	66	DOL
M2	76	VR
M5	90	VR

TABLE IV
MOTOR STARTING PLAN SEQUENCE 2A

Motors-Loads	Connection Bus	Connection Moment (s)
M2	101	10
M5	102	20
M6	103	30
M7 & M9	104	40
M12	105	50
M13	106	60
M14	107	70
M15 & GL	108	80

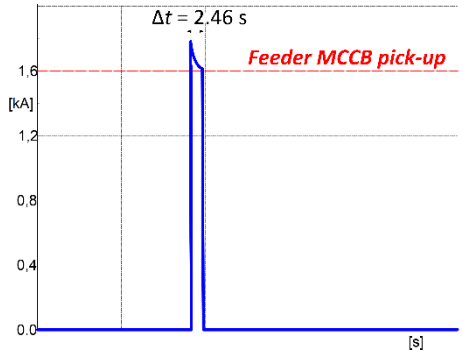

Fig. 9. Start and trip of motors M7 and M9 supplied by feeder 10-104.

These undesired effects are countered with the implementation of a carefully designed motor starting plan following two main drivers: the minimization of the total motor starting plan duration and the limitation of the current and voltage values within acceptable thresholds. In order to achieve this goal, motors that are connected to the same bus are starting in different moments, whereas the rest of the motors are starting with small delays in order to minimize the total duration but also to limit the total generator current as well. The decided motor starting plan sequence (sequence 2b) is displayed in detail in Table V.

By applying the motor starting sequence 2b, the voltage dips are significantly reduced, never becoming lower than 0.94 pu (Fig. 10), while the generator current remains within acceptable limits, below the generator overcurrent protection settings (Fig. 11).

C. Transition to different operational states (G3oS)

The most influencing case in terms of its impact on system voltage and current response is the transition from the MS to the NCS. During this transition, a variety of changes (load connections, disconnections, demand changes) hold, but also some of the motor loads remain completely unchanged. Table VI summarizes all actions concerning motor loads. The impact of the transition from the MS to the NCS on the main bus voltage and generator current are revealed in Fig. 12 and Fig. 13 respectively.

Note that, in general, no serious low voltage problems appear, nor any undesired relay trip is expected during any transition. Hence, the overall operation of the tanker grid is not jeopardized. However, note also that this is due to the fact that the best motor starting method is assumed for each motor and an appropriate starting sequence is also selected.

TABLE V
MOTOR STARTING PLAN SEQUENCE 2B

Motors-Loads	Connection Bus	Connection Moment t (s)
M2	101	5
M5	102	13
GL	108	20
M7	104	23
M6	103	26
M12	105	27
M13	106	28
M14	107	30
M9	104	33
M15	108	36

TABLE VI
TRANSITION FROM MS TO NCS

	Motor Loading Changes (in kW)		Transition Moment t (s)
Motors	**MS**	**NCS**	
M1	90.13	110.92	5
M2	341.77	119.22	10
M3	OUT	86.05	20
M4	OUT	OUT	No change
M5	404.63	430.94	32
M6	OUT	17.4	40
M7	74.34	74.34	No change
M8	OUT	97.87	50
M9	101.02	101.02	No change
M10	126.38	OUT	60
M11	84.26	OUT	70
M12	OUT	OUT	No change
M13	80.40	94.51	80
M14	112.00	112.00	No change
M15	7.5	7.5	No change
Total	**1422.43**	**1251.77**	

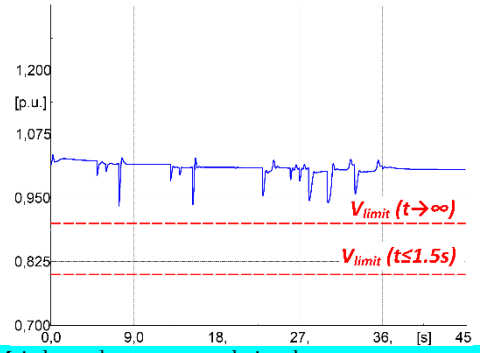

Fig. 10. Main bus voltage response during the motor start sequence 2b.

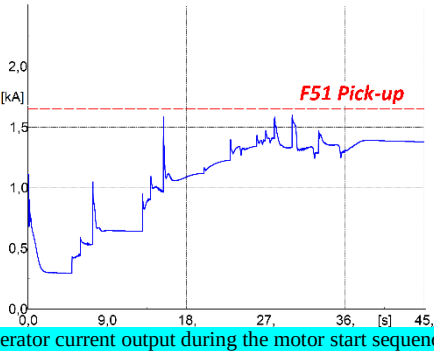

Fig. 11. Generator current output during the motor start sequence 2b.

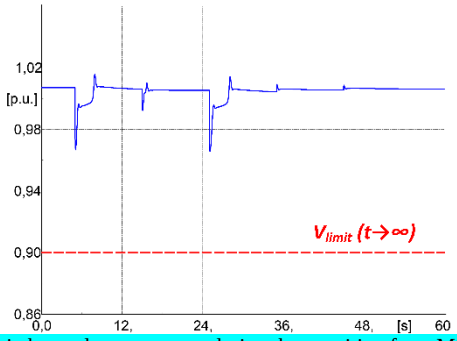

Fig. 12. Main bus voltage response during the transition from MS to NCS.

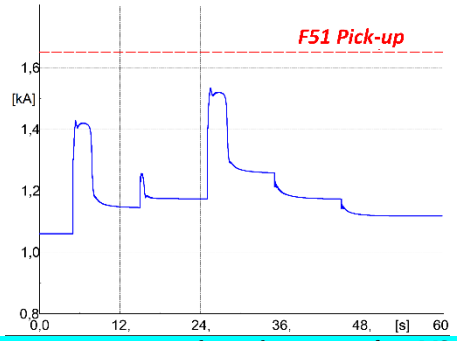

Fig. 13. Generator current output during the transition from MS to NCS.

VI. Conclusions

The paper describes the dynamic behavior of an AC shipboard power system, comprising a significant number of induction motors. It is found from the simulations that voltage collapse is possible when individual high power rated motors start directly-on-load. It is also revealed that during sequential motor starts and motor reacceleration during the transition of one ship's operational state to another, severe voltage drops and overcurrents may appear, endangering the operation of the entire system. Overcurrents should be uniquely studied since it is shown that they may cause undesired overcurrent protection operation, which may trip correctly but undesirably during motor starts or reacceleration. Simulation results show that voltage dip problems can be dealt with by carefully planning an adequate motor starting sequence, which reduces the starting duration and magnitude.

VII. References

[1] M. R. Patel. *Shipboard Electrical Power Systems*. Boca Raton, CRC Press, 2012, p. 339.

[2] J. Prousalidis, E. Styvaktakis, "Introducing a classification method of voltage dips in ship electric energy systems", Journal of Marine Engineering and Technology, 2008.

[3] W. Liuet al., "Impact of the voltage dips in shipboard microgrid power systems," in Proc. 43rd Annu. Conf. Ind. Electron. Soc., 2017, pp. 2287–2292.

[4] Gomez, C. Reineri, G. Campetelli, M. Morcos, "A study of voltage sags generated by induction motor starting, "Elect. Power Compon. Syst., vol. 32, no. 6, pp. 645–653, 2004.

[5] Prousalidis, E. Styvaktakis, E. Sofras, I. K. Hatzilau, D. Muthumuni,"Voltage dips in ship systems," in Proc. Elect. Ship Technol. Symp., 2007,pp. 309–314.

[6] W. Liu, T. Tarasiuk, C.-L. Su, M. Gorniak, M. Savaghebi, J. C. Vasquez, J. M. Guerrero, "An Evaluation Method for Voltage Dips in a Shipboard Microgrid Under Quasi-Balanced and Unbalanced Voltage Conditions", IEEE Transactions on Industrial Electronics, vol. 66, no. 10, Oct. 2019.

[7] A. Anwar, H. Zheng, R. A. Dougal, Y. Zhang, " Fault-Aware-Soft-Restart Method for Shipboard MVAC Power System Using Inverter Coupled Energy Storage System," 2013 IEEE Electric Ship Technologies Symposium (ESTS), Arlington, VA, USA.

[8] H. Awad, J. Svensson, M. Bollen, "Mitigation of unbalanced voltage dips using static series compensator," IEEE Trans. Power Electron., vol. 19, no. 3, pp. 837–846, May 2004.

[9] M. Bongiorno J. Svensson, "Voltage dip mitigation using shunt-connected voltage source converter,"IEEE Trans. Power Electron., vol. 22,no. 5, pp. 1867–1874, Sep. 2007.

[10] P. Kundur. *Power System Control and Stability*. McGraw-Hill Inc., 1994, p. 1200.

[11] Siemens Power Technologies International, "PSS/E Program Application Guide, vol. 2," 2013.

[12] S. E. Zocholl. *AC Motor Protection*. Schweitzer Engineering Laboratories, Inc. 2003, p. 90.

[13] P. Krause, O. Wasynczuk, S. Sudhoff, and S. Pekarek. *Analysis of Electric Machinery and Drive Systems*. John Wiley & Sons, Inc., New Jersey, 2013, p. 659.

[14] Germanischer Lloyd, "Rules and Guidelines - January 2017". [Online]. Available:http://rules.dnvgl.com/docs/pdf/gl/maritimerules/glrp-e.pdf.